Bioinspiration & Biomimetics

PAPER

Algorithmic-driven design of shark denticle bioinspired structures for superior aerodynamic properties

To cite this article: Joshua Ott *et al* 2020 *Bioinspir. Biomim.* **15** 026001

Bioinspiration & Biomimetics

RECEIVED
1 September 2019

REVISED
30 October 2019

ACCEPTED FOR PUBLICATION
27 November 2019

PUBLISHED
10 January 2020

PAPER

Algorithmic-driven design of shark denticle bioinspired structures for superior aerodynamic properties

Joshua Ott, Manuel Lazalde and Grace X Gu[1]

Department of Mechanical Engineering, University of California, Berkeley, CA 94720, United States of America

[1] Author to whom any correspondence should be addressed.

E-mail: ggu@berkeley.edu

Keywords: bioinspired materials design, shark skin denticles, computational fluid dynamics, simulation, computer-aided-design, optimization

Abstract

All engineering systems that move through fluids can benefit from a reduction in opposing forces, or drag. As a result, there is a significant focus on finding new ways to improve the lift-to-drag ratios of systems that move through fluids. Nature has proven to be an extremely beneficial source of inspiration to overcome current technical endeavors. Shark skin, with its low-drag riblet structure, is a prime example of an evolutionary design that has inspired new implementations of drag reducing technologies. Previously, it has been shown that denticles have drag reducing properties when applied to airfoils and other surfaces moving through fluids. Researchers have been able to mimic the structure of shark skin, but minimal work has been done in terms of optimizing the design of the denticles due to the large number of parameters involved. In this work, we use a combination of computational fluid dynamics simulations and optimization methods to optimize the size and shape of shark skin denticles in order to decrease drag. Results show that by changing the size, shape, and orientation of the denticles, the boundary layer can be altered, and thereby reduce drag. This research demonstrates that denticles play a similar role as vortex generators in energizing the boundary layer to decrease drag. These mechanisms, along with the fundamental knowledge gained through the study of these drag reducing structures can be applied to a vast number of fields including aeronautical, oceanic, and automotive engineering.

1. Introduction

Systems moving through fluids experience a resistive force that decreases the efficiency with which the system moves through the fluid. Reducing this resistive force, or drag, increases the efficiency of such systems [1]. This efficiency is commonly measured in terms of the lift-to-drag ratio of the system, with more efficient systems tending to have a higher ratio. As a result, there is a significant focus on finding new ways to improve the lift-to-drag ratio. Nature serves as an inspiration for unique architectures, spurring the field of bioinspired materials to emulate the templates seen in natural materials [1–5]. After all, the evolutionary process produces highly functional and creative designs that can enable improvements to different properties of these individual systems [6–8].

Shark skin is a prime example of an evolutionary design that inspires new implementations of drag reducing technologies [9–15]. Of particular interest is the skin of the fastest swimming shark: the *Isurus oxyrinchus*, otherwise known as the mako shark. Shark skin appears to be smooth but is actually covered with toothlike scales known as denticles [15, 16]. Denticles are composed of two layers: the outer layer and the inner bone structure. The outer layer is made up of an enamel called dentine and the inner layer is a rigid bone structure. Together they form a complex 3D system of ridges [17–19]. The denticles are arranged in a relatively unidirectional pattern. The denticle arrangement and composition causes shark skin to feel smooth when stroked in one direction and coarse when stroked in the other. Unlike the scales of typical marine animals (ctenoid scales) which grow larger as the marine animal grows, denticles remain the same size. The mako shark instead grows more denticles as it grows larger [16]. These denticles decrease drag as the shark moves through water, serving a similar purpose as vortex generators on airplane wings [20–26]. The shape of the denticle delays boundary layer separation in the wake of the denticle, enhancing suction of the fluid flow to the surface the fluid is passing over. Addi-

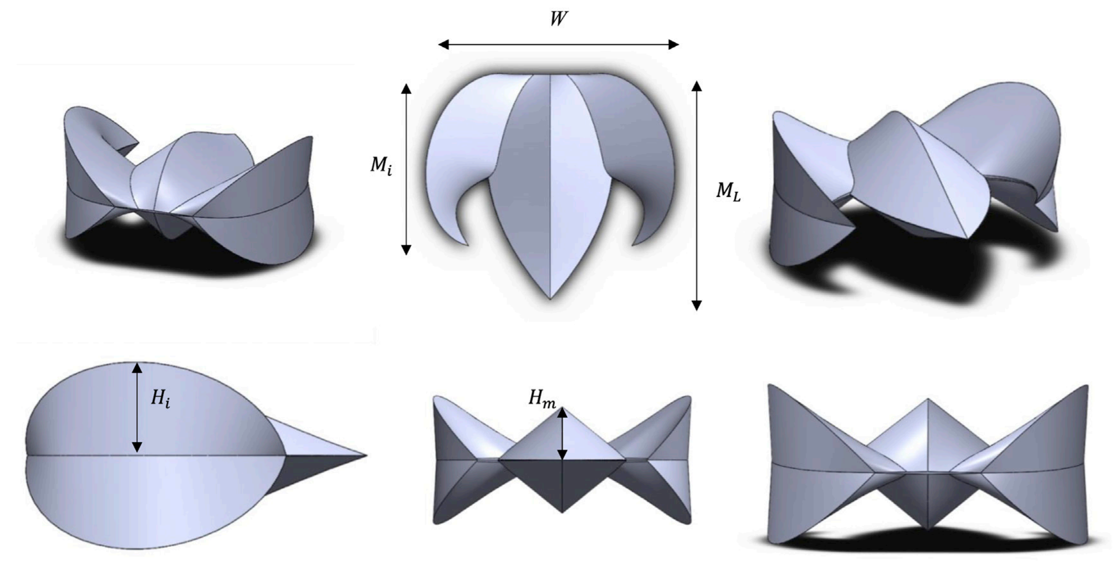

Figure 1. Parameterization of shark skin denticle design with five parameters that influence the length, width, and height of the central body. M_i is the minor length. M_L is the major length. W is the width. H_M is the major height and H_i is the minor height. The first row from left to right shows the isometric view, top view, and rear isometric view. The second row from left to right shows the right-side view, rear view, and front view.

tionally, the denticle creates vortices which help to restore boundary layer momentum losses due to skin friction in the boundary layer, similar to the method in which vortex generators reduce drag on conventional aircraft [27]. On the surface of an airfoil, the denticles are expected to reduce drag and thereby improve the lift to drag ratio. The topic of drag reduction from surface roughness is well studied [25] and is most popularly seen on the surface of golf balls.

The structure of shark skin denticles is currently attracting significant interest from the biological and engineering communities due to the denticle's unique drag reducing properties [28, 29]. Recent efforts involve biologists and engineers studying the realistic effects of 3D-printed denticles on a moveable foil that mimics the motion of sharks. This motion recreates the hydrodynamic environment experienced by sharks in nature [14]. Before this, bioengineering studies of denticles analyzed how surface roughness affects drag [4–6, 13]. As expected, decreasing the surface roughness generally decreases drag for all surfaces. The aerodynamic community is also actively researching denticles [15]. Denticles were analyzed on their ability to passively alter fluid flow around a hydrofoil [27]. Conducting the experiment underwater, researchers found that the hydrofoils with denticles successfully outperformed hydrofoils without denticles due to the way in which denticles acted as vortex generators to delay separation of the boundary layer [27]. Experiments show that denticles reduce drag when tested on airfoils and other mechanisms in water, but significant efforts have not been made in order to optimize the size and shape of the denticles [9–14, 27]. The complex geometry of the denticle consists of several different parameters controlling its size, shape, and orientation. Up to this point, the interplay of these different geometrical features such as length, width, height, and angle of orientation is still unclear in literature due to the large design space.

This paper aims to fundamentally understand how altering these geometric parameters affects the performance of the shark denticle. A combined effort of computational fluid dynamics (CFD) and optimization framework helps to elucidate the effects of the denticle's geometry and orientation on drag, building on the literature focusing on bioinspired design. Significant drag reduction results from optimizing the nume-rous parameters of the denticle design, paving the way for more efficient denticle inspired airfoils and hydrofoils in the future. Section 2 discusses the methods and materials used in this work. Section 3 discusses the results of the CFD and optimization scheme. Finally, section 4 discusses conclusions and future work.

2. Methods

2.1. Parameterization of the shark skin denticle

This paper aims to optimize the geometry of shark skin denticles to understand the fundamental mechanisms through which they alter the surrounding flow. The first step in the process involves creating a solid model of a single denticle using the Computer Aided Design (CAD) tool, SolidWorks®. Once complete, the model is parameterized which involves creating variables for important dimensions in the model. M_i is the minor length, M_L is the major length, H_i is the minor height, H_M is the major height, and W is the width as seen in figure 1. Establishing the boundary conditions in table 1 for these variables is an important part of the process of parameterization, ensuring the geometry is always valid and a solid model can be created from the geometry. An invalid geometry consists of self-intersections and is a nonphysical shape that has

Table 1. Parameterization of the denticle. See figure 1 for corresponding features on the denticle.

	Minor length (M_l)	Major length (M_L)	Width (W)	Major height (H_M)	Minor height (H_l)
Range [mm]	1.25–2.125	1.5–3	2–7.5	0.25–2.5	0.035–1.65

no meaning within the model. Therefore, placing constraints on the five parameters ensures that the geometry does not contain any self-intersections and is therefore always valid—meaning a 3D model can always be created. It is important to note that in this study we have chosen five key parameters that define the shape of the denticle. These five key parameters are a subset of the number of parameters that could be chosen to create a denticle geometry. The five parameters were chosen based on their capacity to influence primary geometrical features of the denticle shape. Other parameters that could be studied in the future include the denticle's angle of orientation to the flow and non-symmetric denticle configurations.

2.2. Reynolds number consideration

With the initial denticle solid model, the Reynolds number range is established so that the denticle model can be properly scaled. The two Reynolds number regimes present in this study correspond to the two separate flow environments that mako sharks and commercial aircraft experience. Commercial aircraft operate in a Reynolds number regime of roughly 10 000–1000 000 from takeoff to landing [3, 27]. The average mako shark denticle of length 0.15 mm [13, 14, 27] has a Reynolds number of roughly 3000. Additionally, the average top speed of a mako shark is between 20 and 27 m s^{-1} [13, 14, 27, 30, 31]. Using the values for the kinematic viscosity of water, V_w [23–25, 30, 31] and the kinematic viscosity of air, V_a [13, 14, 30, 31], along with the Reynolds number equation [30, 31], the Reynolds number is determined to be 2900 with respect to the length of the denticle and 350 000 with respect to a NACA-0012 airfoil with a chord length of 240 mm.

With this Reynolds number range, the appropriate flow speed for the model can be calculated. For practical testing, these structures would be 3D-printed on the surface of an airfoil. Current, 3D-printing resolutions restrict the smallest size of the denticle that could be fabricated. The average size denticle that can be 3D-printed would have a length of 2 mm. Thus, the flow speed would have to be 21.82 m s^{-1} to match the Reynolds number of 350 000. It is important to note that the Reynolds number is calculated across the denticle using the major length because only a small percentage of air particles are traversing the curved path of the denticle. Most of the surrounding air particles are unaffected by the denticle and travel the major length, making this a reasonable approximation in calculating the Reynolds number across the denticle, especially given the scale.

The corresponding airfoil chord length can now be calculated using the proper flow speed and Reynolds number range of the denticle and airfoil. It is important to scale the Reynolds number for both the flow across the airfoil as well as the denticle. This ensures that the flow conditions for both length scales match that of real-world applications. By only focusing on the Reynolds number for the airfoil, the flow across the denticle may not match that experienced by the mako shark in nature. Proper scaling enables matching the Reynolds number of common airfoils used in industry while also matching the Reynolds number that the denticles experience in nature [15].

2.3. Response surface optimization

A computational fluid dynamics (CFD) model is developed once the appropriate flow speed, Reynolds number, and scaled denticle solid model are determined. In particular, ANSYS® Fluent can perform a Response Surface Optimization to find an optimal geometry with the proper CFD model. Figure 2 walks through the process of starting with an initial geometry and then creating a mesh of the denticle geometry. The design of experiments populates the design space based on the specified parameterization constraints. The response surface optimization uses the results from the design of experiments to determine the optimal geometry. Note, all further mentions of 'design of experiments' refers to simulation work. In this case, the objective function of the optimization is to minimize the coefficient of drag. Note that the denticle is placed at a zero-degree angle of attack with respect to the incoming flow, and the coefficient of lift is close to zero at zero angle of attack.

In nature, the denticle itself is on a curved surface (the shark's body), but locally around the denticle it is as if the surface is flat. Because the denticle is significantly smaller than the length scale of the shark's body, the flow around the denticle can be approximated as being at zero angle of attack. Using this assumption and the fact that symmetric objects are expected to produce negligible lifting force at zero angle of attack, we can reasonably focus our attention on minimizing drag. While the ratio of the coefficient of lift to coefficient of drag is still important, changes in the coefficient of lift are two orders of magnitude smaller than changes in the coefficient of drag. Therefore, focusing our attention on drag is of greater interest.

3. Results

3.1. Flow model

The CFD model allows for the coefficient of lift and the coefficient of drag to be calculated across the shark denticle. In particular, the CFD model utilizes a

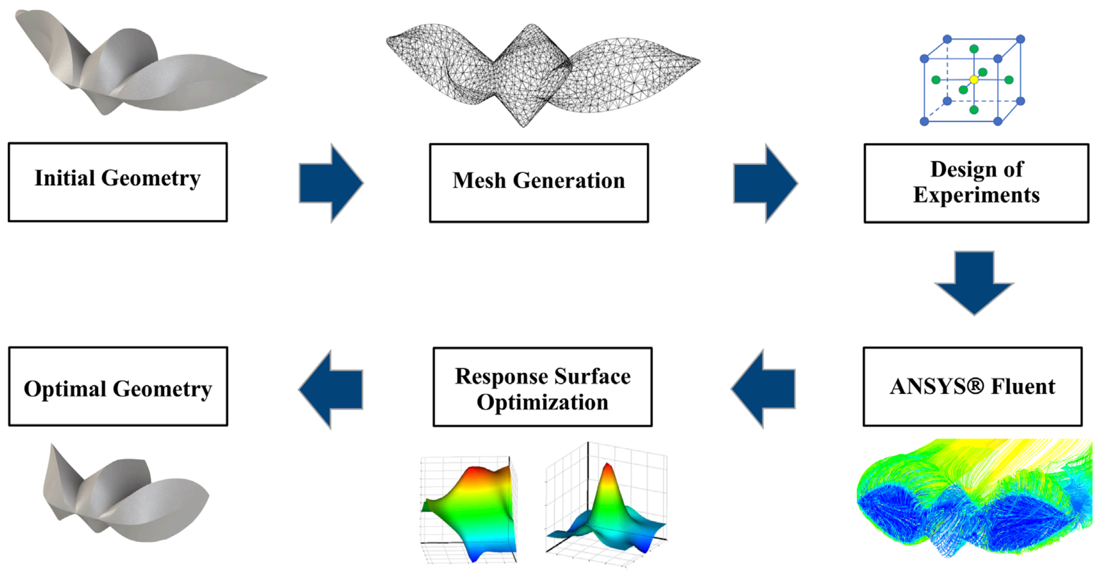

Figure 2. Workflow of research to design shark skin denticles starting from the initial geometry and ending with an optimized geometry. The response surface optimization (RSO) finds the optimal geometry from the design space populated by the design of experiments. The goal for this RSO is to minimize the coefficient of drag.

hybridization of the finite element and finite volume method to discretize the Navier Stokes equations. With the adoption of the shear stress transport (SST) turbulence model, the flow separation across the denticle can accurately be predicted. The SST turbulence model combines the $k - \omega$ model near the surface of the denticle with the $k - \varepsilon$ model further out from the surface of the denticle. This model greatly improves the predictions of adverse pressure gradients, creating a more accurate picture of the flow [26].

3.2. Mesh generation

Besides the methods for solving the flow model, the meshing of the fluid domain is another important factor to consider. The CFD model uses the default mesh parameters inside of a rectangular fluid domain. By deliberately decreasing the mesh size near the surface of the denticle, as well as in the wake of the denticle, the refined mesh guarantees more precise results. Further away from the surface of the denticle, the mesh size increases because less detail is required when solving for the homogenous flow parameters at a greater distance from the surface of the denticle. This process decreases the computational run time without compromising the accuracy of the results. The denticle solid model uses the parameterization shown in figure 1 to vary the size and shape of the denticle. The five parameters reflect the main defining characteristics of the geometry. Upper and lower bounds are placed in order to constrain the design of experiments from producing an invalid geometry with the constraints of the solid modeler. To evaluate the meshing related error in the numerical simulation, mesh sizes from 100 000 to 4 million elements are used. At 3 million mesh elements, a variation in the coefficient of drag of 2×10^{-5} is determined. This corresponds to roughly a 1% error deviation from the calculated coefficient of drag, which is believed to be sufficient for this study.

3.3. Design of experiments

In each design of experiments trial, thirty different denticle geometries are explored with the CFD model. Using the objective function of minimizing the coefficient of drag, the best geometry is selected. Six different design of experiments trials produce six optimal geometries. By averaging the values of the five parameters from the six different trials, the optimized geometry is determined. Note that some of the trials perform better than the overall optimized geometry since the average is taken over the six trials. Figure 3 depicts the results of one trial with certain selected geometries. An outlier geometry is denoted as Design 1. A geometry that has a similar structure to the optimized geometry is denoted as Design 2. The optimized design is denoted as the Optimized Design.

There are also striking trends to notice across the various trials. For example, the coefficient of lift is two orders of magnitude smaller than the coefficient of drag. This discrepancy is expected because the denticle is symmetric, producing negligible amounts of lift at zero degrees angle of attack. Figure 3 presents the pressure contour comparison for three different stages of the response surface optimization process. The optimal geometry should have a smaller frontal area to reduce drag. Additionally, the central body of the optimal geometry should become more oblong to produce a greater defined streamlined shape. The trials confirm this expectation and illustrate that the high-pressure area on the front of the denticle is greatly reduced. Also, the two wing-shaped structures of the denticle do not have drastic changes due to the choice of parameters

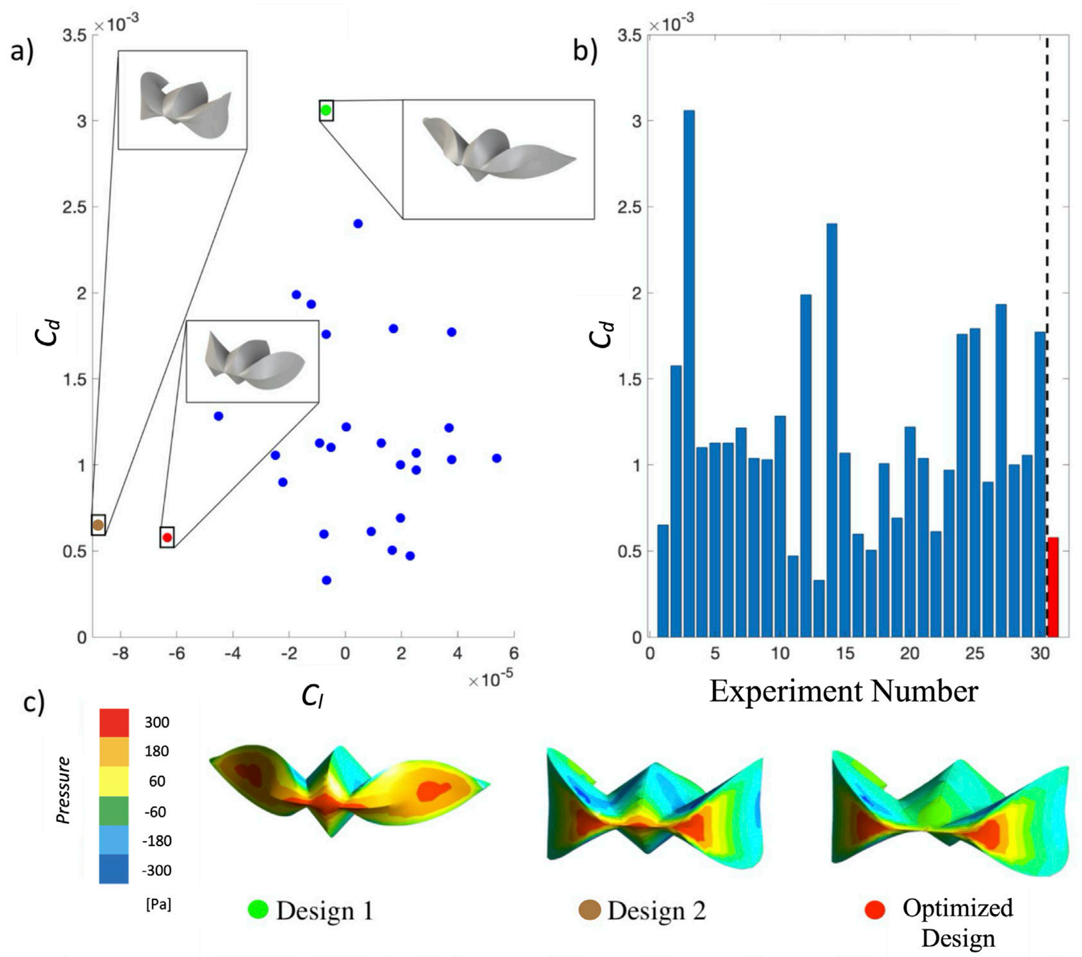

Figure 3. (a) and (b) Results from one of the six trials in the optimization process. The overall optimized geometry which is averaged from all six trials is shown in red. (c) Pressure contours comparison from three different stages of the response surface optimization process.

for the denticle. These wing structures are an integral part of the denticle geometry involved with vortex generation, aiding in energizing the boundary layer to delay separation. Thus, it is imperative to maintain the integrity of the wing-shape structures in order to preserve the inherent nature of the denticles. Again, note that the average value for the five key geometric parameters are taken from the results of six trials due to the small variation ANSYS reports in calculating the coefficient of lift and drag. This variation in the coefficient of lift and drag is expected from all computational fluid dynamics solvers, especially when using turbulence models. This explains why some geometries appear to outperform the overall optimized geometry. However, the average optimized geometry robustly outperforms the other designs when accounting for the variations caused by the turbulence model.

Previous studies indicate that geometric disturbances within the boundary layer can produce vortices which energize the boundary layer and lead to a delay in separation [27]. The vortices bring fluid from the outer part of the boundary layer with greater momentum closer to the surface, where the negative effects of skin friction are the greatest. This separation delay decreases the amount of drag experienced by the object. As can be shown in figure 4, the denticle acts as a vortex generator by producing vortices to energize the boundary layer in their wake. Further optimization is required to determine the optimal spacing of denticles on the surface of an airfoil in order to achieve the greatest effect from this vortex generation.

3.4. Drag reduction

Comparing different geometries generated by the design of experiments enables unique insight into the inherent nature of the denticle. The same denotations and designs are displayed in both figures 3 and 4. The first row of figure 4 indicates that the shear experienced at the upper surface of the denticle is similar between the Optimized Design and Design 2. However, the separation occurs further back on the Optimized Design as expected, which is apparent from the spiral forming at the rear of the denticle. In Design 1, the separation occurs even further ahead than Design 2 due to the large frontal area of the design. In the second row, the velocity contours are shown at a plane equally spaced in the wake of each denticle. There is a significant difference between Design 2 and the Optimized Design. Because the Optimized Design has a significant reduction in frontal area, the velocity

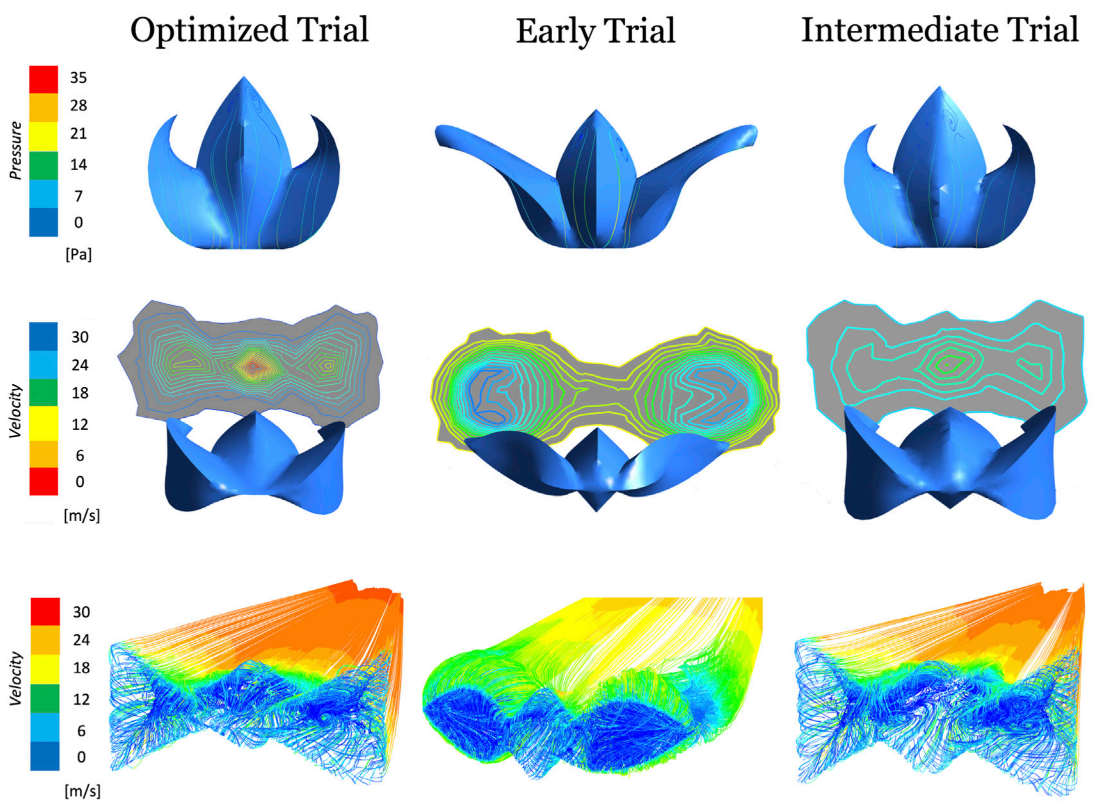

Figure 4. Comparison of pressure and velocity profiles in different designs. The first row indicates the shear at the surface of the denticle from the top view. Note that the separation occurs further to the rear of the denticle on the Optimized Design compared to Design 1 and Design 2. The second row displays the velocity contours on a fixed plane at equal distance in the wake of each design. Note that the velocity of the wake of the Optimized Design is the greatest. Finally, the third row shows the velocity streamlines around the structure of the denticle designs. The velocity in the wake of the Optimized Design is greatest due to the reduction in frontal area of the denticle as well as the more defined oblong shape.

at the plane for the Optimized Design is greater than the velocity at the plane for Design 2. Additionally, Design 1's velocity at the plane behind the two large wing structures is relatively low. These two large wing structures act as significant hindrances to the flow, producing a large amount of drag. Finally, the third row captures the streamlines around the denticle geometries. In the wake of the Optimized Design, there is far less disturbance than in both Design 1 and Design 2. Additionally, the mean velocity in the wake of the Optimized Design is significantly higher than the corresponding mean velocity in the wake of Design 1 and Design 2 as a result of the reduced drag across the optimal design.

Figures 3 and 4 demonstrate that despite the similar structure between Design 2 and the Optimized Design, there is a significant difference in performance. This difference indicates the need for optimization. The decrease in frontal area combined with the oblong shape of the Optimized Design allows the Optimized Design to consistently outperform Design 1 and Design 2. By optimizing the size and shape of the denticle geometry, there is a fundamental improvement in the aerodynamic performance of the denticle. This paper takes the product of evolution and applies modern optimization techniques to determine the best performing geometry given an objective function. Similar improvements can be achieved in aquatic, aeronautic, and automotive applications by applying the knowledge gained from the optimization of these fundamental mechanisms to reduce drag and therefore increase efficiency and decrease overall cost.

4. Conclusions and future work

This work explores optimal designs of the shark denticle to decrease drag and optimize aerodynamic performance. A computational model paired with a response surface optimization allowed for the determination of the optimal geometry. This research demonstrates that denticles play a similar role as vortex generators in energizing the boundary layer to decrease drag. It was shown that too much disruption of the flow leads to large amounts of drag, but through optimization, the best design can be selected in order to maximize performance. The necessity for optimization in the size and shape of the denticle is demonstrated by significant improvements from creating a more streamlined shape. Through this optimization method, denticles can be further utilized as an essential tool in drag reduction. Future work will apply the denticles to the surface of an airfoil. Therefore, it is important to first create the optimal geometry with respect to the flow that the denticle will experience locally. This is why the denticle was simulated separately from the surface of an airfoil. Future research also involves exploring the pairing of our design of experiments with machine learning techniques [32–37] to further enhance our optimization method. Additional work will be performed to additively manufacture and experimentally test denticle configurations in wind tunnels to compare different designs of denticles.

Acknowledgments

The authors acknowledge support from the Regents of the University of California, Berkeley and the Extreme Science and Engineering Discovery Environment (XSEDE) Bridges system at the Pittsburgh Supercomputing Center (PSC) through allocation TG-DMR180085, which is supported by National Science Foundation Grant No: ACI-1548562. The authors also acknowledge support from the Savio computational cluster resource provided by the Berkeley Research Computing program. Additionally, the authors would like to thank Richard Didham, Zachary Sorscher, and Michael Neufer for insightful discussions.

ORCID iDs

Joshua Ott https://orcid.org/0000-0002-6754-8316
Grace X Gu https://orcid.org/0000-0001-7118-3228

References

[1] Studart A R 2013 Biological and bioinspired composites with spatially tunable heterogeneous architectures *Adv. Funct. Mater.* **23** 4423–36
[2] Wegst U G, Bai H, Saiz E, Tomsia A P and Ritchie R O 2015 Bioinspired structural materials *Nat. Mater.* **14** 23–36
[3] Gu G X, Libonati F, Wettermark S D and Buehler M J 2017 Printing nature: unraveling the role of Nacre's mineral bridges *J. Mech. Behav. Biomed. Mater.* **76** 135–44
[4] Gu G X *et al* 2016 Three-dimensional-printing of bio-inspired composites *J. Biomech. Eng.* **138** 021006
[5] Gu G X, Takaffoli M and Buehler M J 2017 Hierarchically enhanced impact resistance of bioinspired composites *Adv. Mater.* **29** 1700060
[6] Bar-Cohen Y 2005 *Biomimetics* (Boca Raton, FL: CRC Press) pp 495–513
[7] Benyus J M 1997 Biomimicry *Innovation Inspired by Nature* (New York, NY: Harper Collins)
[8] Patek S N 2014 Biomimetics and evolution *Science* **345** 1448–9
[9] Dean B and Bhushan B 2010 Shark-skin surfaces for fluid-drag reduction in turbulent flow: a review *Phil. Trans. R. Soc.* A **368** 4775–806
[10] Fu Y F, Yuan C Q and Bai X Q 2017 Marine drag reduction of shark skin inspired riblet surfaces *Biosurface Biotribol.* **3** 11–24
[11] Sareen A, Deters R W, Henry S P and Selig M S 2014 Drag reduction using riblet film applied to airfoils for wind turbines *J. Sol. Energy Eng.* **136** 021007
[12] Oeffner J and Lauder G V 2012 The hydrodynamic function of shark skin and two biomimetic applications *J. Exp. Biol.* **215** 785–95
[13] Lauder G V, Wainwright D K, Domel A G, Weaver J C, Wen L and Bertoldi K 2016 Structure, biomimetics, and fluid dynamics of fish skin surfaces *Phys. Rev. Fluids* **1** 1044
[14] Wen L, Weaver J C and Lauder G V 2014 Biomimetic shark skin: design, fabrication and hydrodynamic function *J. Exp. Biol.* **217** 1656–66
[15] Domel G *et al* 2018 *Bioinspir. Biomim.* **13** 056014
[16] Liem K F, Bemis W E, Walker W F and Grande L 2001 *Functional Anatomy of the Vertebrates. An Evolutionary Perspective* 3rd edn (Fort Worth, TX: Harcourt College Publishers)
[17] Castro J I 2011 *The Sharks of North America* (Oxford: Oxford University Press)
[18] Reif W E 1982a Morphogenesis and function of the squamation in sharks *Neues Jahrb. Geol. Palaontol. Abh.* **164** 172–83
[19] Reif W-E and Dinkelacker A 1982 Hydrodynamics of the squamation in fast swimming sharks *Neues Jahrb. Geol. Palaontol. Abh.* **164** 184–7
[20] Lin J C, Howard F G and Selby G V 1990 Small submerged vortex generators for turbulent flow separation control *J. Spacecr. Rockets* **27** 503–7
[21] Lin J C 2002 Review of research on low-profile vortex generators to control boundary-layer separation *Prog. Aerosp. Sci.* **38** 389–420
[22] Yao C, Lin J and Allen B 2002 Flowfield measurement of device-induced embedded streamwise vortex on a flat plate *1st Flow Control Conf.* (Reston, VA: American Institute of Aeronautics and Astronautics)
[23] Kerho M, Hutcherson S, Blackwelder R F and Liebeck R H 1993 Vortex generators used to control laminar separation bubbles *J. Aircr.* **30** 315–9
[24] Lin J C, Robinson S K, McGhee R J and Valarezo W O 1994 Separation control on high-lift airfoils via micro-vortex generators *J. Aircr.* **31** 1317–23
[25] Lin J 1999 Control of turbulent boundary-layer separation using micro-vortex generators *30th Fluid Dynamics Conf.* (Reston, VA: AIAA)
[26] Storms B L and Jang C S 1994 Lift enhancement of an airfoil using a Gurney flap and vortex generators *J. Aircr.* **31** 542–7
[27] Domel A G, Saadat M, Weaver J C, Haj-Hariri H, Bertoldi K and Lauder G V 2018 Shark skin- inspired designs that improve aerodynamic performance *J. R. Soc. Interface* **15** 20170828
[28] Büttner C C and Schulz U 2011 Shark skin inspired driblet structures as aerodynamically optimized high temperature coating for blades of aeroengines *Smart Mater. Struct.* **20** 094016
[29] Mollendorf J C, Termin A C, Oppenheim E and Pendergast D 2004 Effect of swim suit design on passive drag *J Med Sci Sports Exercise* **36** 1029–35
[30] Graham J B *et al* 1990 Aspects of shark swimming performance determined using a large water tunnel *J. Exp. Biol.* **151** 175–92
[31] Díez G, Soto M and Blanco J M 2015 Biological characterization of the skin of shortfin mako shark *Isurus oxyrinchus* and preliminary study of the hydrodynamic behaviour through computational fluid dynamics *J. Fish Biol.* **87** 123–37
[32] Michalski R S, Carbonell J G and Mitchell T M 2013 *Machine Learning: an Artificial Intelligence Approach* (Berlin: Springer)
[33] Pilania G, Wang C, Jiang X, Rajasekaran S and Ramprasad R 2013 Accelerating materials property predictions using machine learning *Sci. Rep.* **3** 2810
[34] Chen C-T and Gu G X 2019 Machine learning for composite materials *MRS Commun.* **9** 556–66
[35] Gu G X, Chen C-T, Richmond D J and Buehler M J 2018 Bioinspired hierarchical composite design using machine learning: simulation, additive manufacturing, and experiment *Mater. Horizons* **5** 939–45
[36] Gu G X, Chen C-T and Buehler M J 2018 De novo composite design based on machine learning algorithm *Extreme Mech. Lett.* **18** 19–28
[37] Liu R *et al* 2015 A predictive machine learning approach for microstructure optimization and materials design *Sci. Rep.* **5** 11551